Journal of proteome research

Article

pubs.acs.org/jpr

Characterization of Phosphorylation- and RNA-Dependent UPF1 Interactors by Quantitative Proteomics

Valentin Flury,[†,§] Umberto Restuccia,[‡] Angela Bachi,[‡] and Oliver Mühlemann*[,†]

[†]Department of Chemistry and Biochemistry, University of Bern, Freiestr. 3, Bern 3012, Switzerland

[‡]IFOM-FIRC Institute of Molecular Oncology Foundation, Via Adamello 16, Milan 20139, Italy

Supporting Information

ABSTRACT: Human up-frameshift 1 (UPF1) is an ATP-dependent RNA helicase and phosphoprotein implicated in several biological processes but is best known for its key function in nonsense-mediated mRNA decay (NMD). Here we employed a combination of stable isotope labeling of amino acids in cell culture experiments to determine by quantitative proteomics UPF1 interactors. We used this approach to distinguish between RNA-mediated and protein-mediated UPF1 interactors and to determine proteins that preferentially bind the hypo- or the hyper-phosphorylated form of UPF1. Confirming and expanding previous studies, we identified the eukaryotic initiation factor 3 (eIF3) as a prominent protein-mediated interactor of UPF1. However, unlike previously reported, eIF3 binds to UPF1 independently of UPF1's phosphorylation state. Furthermore, our data revealed many nucleus-associated RNA-binding proteins that preferentially associate with hyper-phosphorylated UPF1 in an RNase-sensitive manner, suggesting that UPF1 gets recruited to mRNA and becomes phosphorylated before being exported to the cytoplasm as part of the mRNP.

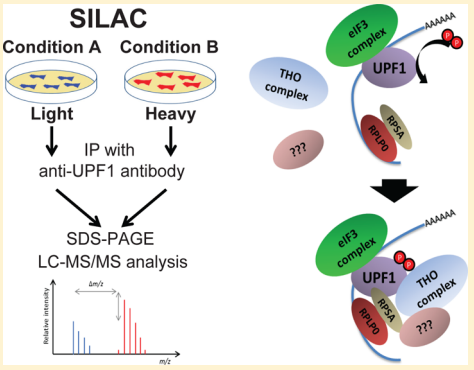

KEYWORDS: *SILAC, NMD, UPF1, RENT1, eIF3, THO complex, TREX, STRAP, UNRIP*

INTRODUCTION

RNA helicases comprise a large family of conserved proteins that bind or remodel RNA or RNA−protein complexes in an ATP-dependent fashion and thereby exert important functions on RNA metabolism.[1] The protein UPF1 (also known as RENT1 or hSMG2) belongs to the superfamily 1 of ATP-dependent helicases and is best known for its key role in nonsense-mediated mRNA decay (NMD), a eukaryotic mRNA turnover mechanism that specifically recognizes and degrades mRNAs on which the termination codon is located in an unfavorable environment for efficient translation termination.[2,3] Besides the classical NMD substrates with prematurely truncated ORFs, 5−10% of all cellular mRNAs change in levels upon inactivation of NMD, indicating that NMD serves as both a quality control and a gene regulatory process.[4] NMD is omnipresent among eukaryotes, and at least three NMD factors, UPF1, UPF2, and UPF3, are conserved between *S. cerevisiae* and *H. sapiens*, with UPF1 showing the highest degree of conservation (48.5% amino acid sequence identity[5]). The three proteins form a complex that stimulates the helicase activity of UPF1.[6] Additional NMD factors are present in metazoans, including the UPF1 phosphorylating kinase SMG1, its regulators SMG8 and SMG9, as well as the 14−3−3-like proteins SMG5, SMG6, and SMG7, that have been reported to preferentially interact with hyper-phosphorylated (p)UPF1 and promote its PP2A-dependent dephosphorylation.[7−12] When recruited to pUPF1-bound mRNA, SMG5 and SMG7 are believed to trigger the exonucleolytic decay of the targeted mRNA by engaging the decapping complex and deadenylases,[13−15] whereas the endoribonuclease SMG6 directly cleaves the mRNA.[16,17]

The key role of UPF1 in NMD is documented by the requirement of its cyclic phosphorylation−dephosphorylation, its ATP binding, ATP hydrolysis, and unwinding activities.[12,18−20] However, the precise molecular pathway of NMD, in particular, the temporal order of the protein−protein and protein−RNA interactions, is not yet completely understood. It is likely that additional yet unknown factors might be involved and possibly associated with UPF1 at some point. Moreover, UPF1 appears to be a truly multitasking enzyme (reviewed in ref 21): in addition to its role in NMD, it is also involved in other cellular processes including Staufen1-mediated mRNA decay (SMD),[22] histone mRNA turnover,[23] telomere maintenance,[24] and cell cycle progression and genome stability.[25] To date, only limited biochemical information is available with regards to the exact role of UPF1 in these additional processes.

As a starting point to gain more insight into the diverse UPF1 functions, we sought for an unbiased way to identify proteins specifically associated with UPF1 and quantify their relative association ratios under different conditions. To distinguish UPF1-specific interactors from unspecifically copurifying proteins, we used a quantitative approach based

Received: March 4, 2014

   dx.doi.org/10.1021/pr5002143 | *J. Proteome Res.* XXXX, XXX, XXX−XXX

on stable isotope labeling by amino acids in cell culture (SILAC)[26] and first compared the proteins immunoprecipitating with an anti-UPF1 antibody with a control IP in which the antibody::UPF1 interaction was prevented by an epitope-binding peptide. Next, we separated RNase-insensitive UPF1 interactors from the RNA-mediated interactors, and finally we identified proteins that differentially associated with UPF1 depending on its phosphorylation state. The results from these analyses revealed both known and novel interactors.

MATERIALS AND METHODS

SILAC Cell Culture Medium

HeLa cells were grown at 37 °C, 5% CO_2 in SILAC media, containing a formula of DMEM/Ham's F12 (without the amino acids L-glutamine, L-arginine, and L-lysine; BioConcept), supplemented with 0.51 mM L-lysine (either heavy: 99% $^{13}C_6{}^{15}N_2$-labeled L-lysine 2HCl [K8; Cambridge Isotope Laboratories] or light: L-lysine HCl [K0; BioConcept]), 0.345 mM L-arginine (either heavy: 99% $^{13}C_6{}^{15}N_4$-labeled L-arginine HCl [R10; Cambridge Isotope Laboratories] or light: L-arginine HCl [R0; BioConcept]), and 0.25 mM L-proline (BioConcept) to avoid arginine-to-proline conversion.[27] This medium was further supplemented with 10% (v/v) dialyzed fetal calf serum (BioConcept), 100 U/mL penicillin, and 100 μg/mL streptomycin and 2 mM L-glutamine.

Immunoprecipitation of UPF1 from Cell Lysates

HeLa cells were grown for at least six cell doublings in heavy or light medium before harvesting. For immunoprecipitation (IP) experiments, 2 to 3 × 10^7 cells were harvested, counted, spun down (5 min at 200*g* and 4 °C), and washed twice with PBS. Cells were lysed in hypotonic gentle lysis buffer (10 mM Tris Base, 10 mM NaCl, 2 mM EDTA, 0.5% Triton X-100, supplemented with protease/phosphatase inhibitor cocktail [ThermoScientific]) to a final concentration of 2 × 10^4 cell equivalents/μL and incubated for 10 min on ice. After centrifugation (15 min, 16 000*g*, 4 °C), the supernatant was transferred to a fresh Eppendorf tube, and 5 M NaCl was added to a final concentration of 150 mM. Proteins were quantified using the Micro BCA Protein Assay Kit (ThermoScientific), equal amounts of protein were transferred to a new Eppendorf tube, and antibodies were added (between 15−20 μg goat α-RENT1 antibody per condition, BETHYL A300-038A). The mixture was incubated for 1.5 h at 4 °C on a rotating wheel. 150−200 μL of Dynabeads Protein G (Life Technologies) per condition (ratio 10:1 μL/μg antibody) were washed three times in wash buffer (137 mM NaCl, 20 mM Tris Base, 0.05% (v/v) Tergitol-type NP-40), washed once in hypotonic gentle lysis buffer, and incubated for 1 h on a rotating wheel at 4 °C. Thereafter, the unbound fraction was saved for analysis, and the beads were washed three times using wash buffer (with protease/phosphatase inhibitor). Beads-bound proteins were eluted with 40 μL of 2× SDS loading buffer, and aliquots of each sample were analyzed by Western blotting. For the preparative gel, the heavy and light eluates were combined and electrophoresed on an 8% SDS-PAGE, stained with Coomassie and stored in 1% acetic acid prior to MS/MS analysis.

MS/MS analysis

Single gel lanes were cut into 12 slices, each of which was processed for trypsin digestion, as previously described.[28] Tryptic digests were further desalted and concentrated using a homemade C18 tip, as described elsewhere,[29] and finally resuspended in 14 μL of 10% formic acid. Five μL of the peptide mixture was analyzed twice as technical replicates and resolved on a 15 cm long homemade C18 column (75 μm inner diameter), filled with Reprosil-Pur C18 3 μm resin (Dr. Maisch, Ammerbuch-Entringen, Germany), using a 70 min long gradient, ramping from 10 to 35% of solvent B (80% acetonitrile, 0.5% acetic acid in water) in solvent A (2% acetonitrile, 0.5% acetic acid in water). Eluting peptides were directly infused into a LTQ-Orbitrap mass spectrometer (Thermo Scientific). Full scans were acquired at high resolution (R = 60 000 @400 m/z), and AGC target was set to 1 × 10^6 at a maximum injection time of 500 ms. The 10 most intense peaks were automatically selected, fragmented by CID set at 37, and acquired in the linear ion trap at low-resolution, AGC target 1 × 10^4, and three microscans of 150 ms each. Ions acquired twice were dynamically excluded for further selection and fragmentation for 90 s. Spectra were loaded into MaxQuant software (v. 1.2.2.5) and searched against the human Uniprot complete proteome set (release 06_2012, 86 875 entries) using the Andromeda search engine.[30] Search parameters were as follows: trypsin strict specificity for cleavage, carbamidomethylation as fixed modification, methionine oxidation, and protein N-terminal acetylation as variable modifications, two missed cleavages allowed, 10 ppm tolerance for the precursor, and 0.5 Da tolerance for the fragment ions. To be considered as identified, proteins had to pass the following criteria: minimum peptide length of 6, at least 2 assigned peptides, and 1 unique peptide. The false discovery rate for both peptides and proteins was set at 0.01. Keratins and proteins derived from fetal calf serum have been removed from further analysis. SILAC quantification was done according to the MaxQuant algorithm, on razor and unique peptides (= most likely belonging to the same protein group), with at least 1 ratio count. Statistical analysis was performed using Perseus tools available in the MaxQuant environment.

The .raw MS files and search/identification files obtained with MaxQuant have been submitted to PeptideAtlas (http://www.peptideatlas.org/, data set identifier PASS00438), and Supplementary Table S1 in the Supporting Information provides the complete protein identification and quantitation table comprising all six experiments.

Western Blot Analysis

For input and unbound fractions, material corresponding to 2 × 10^5 cells and 10% of the elution were electrophoretically separated on a 8% SDS-PAGE (6% for detection of SMG1), transferred on a Optitran BA-S 85 reinforced nitrocellulose membrane (Schleicher and Schuell) and probed as indicated with the following primary antibodies: polyclonal goat anti-hUPF1 (A300−038A, BETHYL, 1:3000 diluted), monoclonal mouse anti-hSMG1 (sc-135563, Santa Cruz Biotechnology, 1:250), monoclonal mouse anti-OctA (Flag, sc-81593, Santa Cruz Biotechnology, 1:1000), polyclonal rabbit anti-hUPF2 (kindly provided by J. Lykke-Andersen, 1:3000), polyclonal rabbit anti hUPF3B (kindly provided by J. Lykke-Andersen, 1:2500), polyclonal rabbit anti-CPSF73 (kindly provided by W. Keller, 1:3000), polyclonal rabbit anti-Act B (A5060, Sigma-Aldrich, 1:3000), polyclonal rabbit anti-p(Ser/Thr) ATM/ATR (2851, Cell Signaling, 1:1000), monoclonal mouse anti-PABPC1 (10E10, sc-32318, Santa Cruz Biotechnology, 1:1000), polyclonal rabbit anti-STRAP (kindly provided by U. Fischer, 1:1000), and polyclonal rabbit anti-UNR (kindly provided by U. Fischer, 1:500). 1:10 000 diluted donkey

dx.doi.org/10.1021/pr5002143 | J. Proteome Res. XXXX, XXX, XXX−XXX

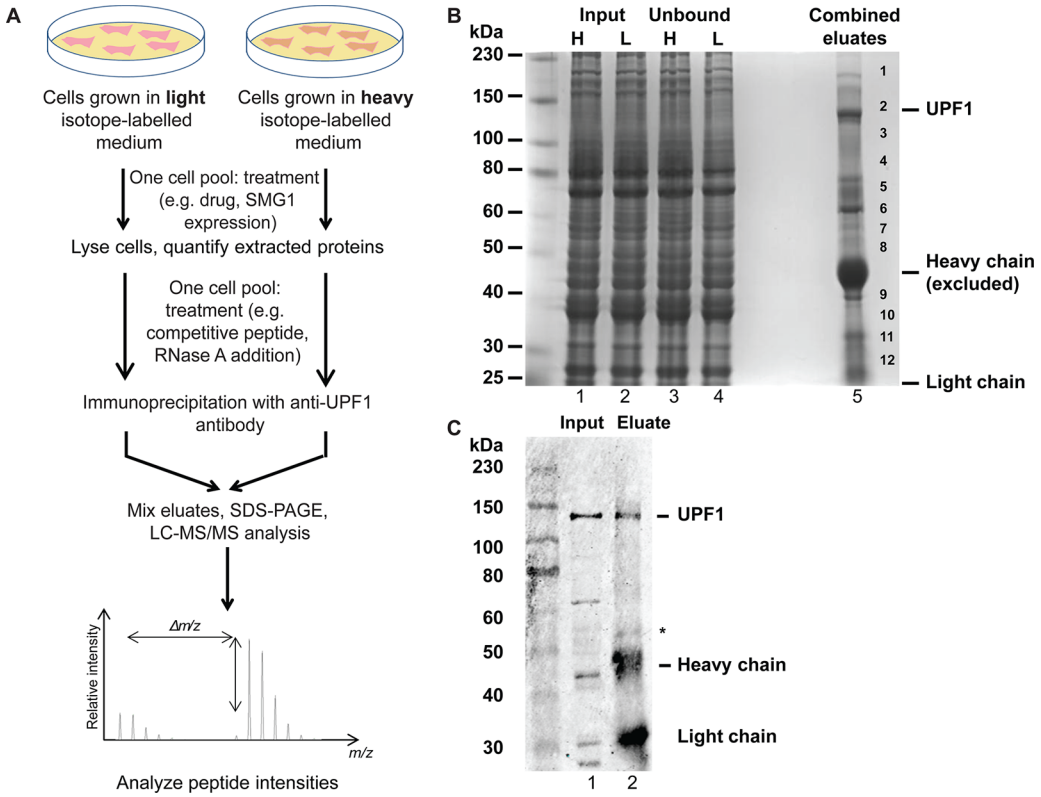

Figure 1. SILAC workflow and monitoring of the immunoprecipitation (IP). (A) Schematic representation of the workflow for the identification of UPF1 interactors. After growing HeLa cells in heavy (H) or light (L) amino-acid-containing media for at least six doublings, one of the cell pools (designated as "experimental sample") received the indicated treatment (e.g., SMG1 expression and addition of OA), while the other cell pool (designated as "reference sample") remained untreated. Cells were then lysed, protein concentrations were quantified, and equal protein amounts were used for IP with an anti-UPF1 antibody. Co-immunopurified proteins of both samples were mixed in a 1:1 ratio, separated by SDS-PAGE and analyzed by liquid chromatography tandem mass spectrometry (LC−MS/MS). (B) Coomassie-stained polyacrylamide gel showing a fraction of the cell lysates (lanes 1, 2) and the unbound material (lanes 3, 4) from an H- and L-labeled sample pair and the combined eluates from these samples after IP with anti-UPF1 antibody (lane 5), from which the indicated bands (1−12) were excised. Proteins in the gel pieces were reduced, alkylated, digested with trypsin, and subjected to LC−MS/MS analysis. Because of the high abundance of the heavy and light chains of the antibody, these regions were excluded from the analysis. (C) The anti-UPF1 antibody (Bethyl A300-038A) immunoprecipitates UPF1 with high specificity. Western blot analysis shows the specific immunoprecipitation of UPF1 (lane 2), whereas additional proteins recognized in HeLa cell lysate are not immunoprecipitated (compare bands in lanes 1 and 2), indicating the unspecific recognition of those proteins only in their denatured but not in their native conformation. The band marked by an asterisk most likely represents the bead-coupled IgG-binding protein G (57 kDa), small amounts of which eluted from the beads during heat denaturation and are recognized by the IgG antibody.

antibody, directed against the species of the first antibody and coupled to IRDye800CW (green, LI-COR) or IRDye680CW (red, LI-COR), was used as secondary antibody. The bands were visualized by scanning the membrane on an Odyssey Infrared Imager (LI-COR). For detection of phosphorylated residues, membranes were blocked and incubated with the indicated antibodies in TBST, 3% BSA, and 10 mM glycerol-2-phosphate to avoid dephosphorylation.

Cell Culture and Transfections in Knockdown Experiments

Knockdown experiments were performed as previously described.[31] For transfections in six-well plates, 2×10^5 cells were seeded in 2 mL of medium per well and transfected the next day with 100 ng of reporter plasmids, 400 ng of pSUPERpuro plasmid,[32] and 3 μL of DreamFect (OZ Biosciences) according to the manufacturer's protocol. One day later, cells were exposed to 1.5 mg/mL puromycin for 2 days and thereafter cultured in antibiotic-free media for another day before total RNA was isolated and whole cell lysates for immunoblotting were prepared. Total cellular RNA was isolated using TRI-reagent.

Plasmids

For the knockdowns, short hairpin RNAs (shRNA) encoded on the pSUPERpuro plasmid[32] were expressed. The shRNA target sequences are provided in the Supporting Information. In the pβminiμ plasmids, the miniμ reporter gene transcripts are driven by the human β-actin promoter.[33] Human SMG1 (NCBI RefSeq NM_015092.4) was cloned into pCK-vector with a N-terminal Flag tag.

Reverse-Transcription-Coupled Quantitative Real-Time PCR (RT-qPCR)

RT-qPCR was performed as previously described.[31] Sequences of primers and TaqMan probes are provided in the Supporting Information.

Flag Co-Immunoprecipitation

For FLAG-based IPs, 2×10^6 cells were seeded and transfected the next day with 2 μg pCK-FLAG-STRAP, pCK-FLAG-GFP, or pCK-FLAG-UPF1 (for UPF1, 3 μg plasmid) using Dreamfect according to the manufacturer's manual. Two days post transfection, cells were washed and harvested in DMEM +/+. Cells were centrifuged (5 min, 200g, 4 °C), washed with

dx.doi.org/10.1021/pr5002143 | J. Proteome Res. XXXX, XXX, XXX−XXX

PBS, centrifuged (5 min, 200*g*, 4 °C), and lysed in an appropriate volume of hypotonic gentle lysis buffer (including protease/phosphatase inhibitors) for 10 min on ice. Afterward, the cell lysate was centrifuged (15 min, 16 000*g*, 4 °C), and the supernatant was transferred to a new Eppendorf tube. 50 μL was set aside for input control analysis. For each IP, 30 μL of anti-FLAG M2 affinity gel slurry (Sigma-Aldrich) was washed with 1 mL of TBS-light (2.5 mM Tris (pH 7.5), 150 mM NaCl). The beads were gently spun down (5 min, 1000*g*, 4 °C), and the supernatant was removed. This washing step with 1 mL of TBS-light was repeated, followed by two washes with 1 mL of glycine 0.1 M, pH 3.5 to remove unbound antibody and a final wash with 1 mL of TBS. The beads were carefully resuspended in hypotonic gentle lysis buffer and added to the lysates. RNase A (Sigma-Aldrich) was added to a final concentration of 200 μg/mL, and the suspension was incubated on a rotating wheel for 2.5 h at 4 °C. The unbound fraction was removed and stored at −20 °C for analysis. The beads were washed once with 1 mL of hypotonic gentle lysis buffer and three times with 1 mL of washing buffer, each followed by a centrifugation step (5 min, 1000*g*, 4 °C), then transferred to a new Eppendorf tube. The proteins were eluted in 60 μL of 2× SDS loading buffer.

RESULTS

Setup of SILAC Experiments

To identify proteins that interact with UPF1 and further characterize (i) whether the interaction is RNA-mediated or occurs through protein−protein contacts and (ii) whether the identified factors exhibit differential binding depending on the phosphorylation status of UPF1, we established the following pairwise SILAC workflows (Figure 1A): HeLa cells were grown for at least 8 days in media, containing either natural (referred to as light) or ^{13}C- and ^{15}N-containing (referred to as heavy) isotopes of L-arginine and L-lysine to allow for complete proteome labeling (Supplementary Figure S1 in the Supporting Information). After cell lysis, equal amounts of total protein from the two to-be-compared experimental conditions were immunoprecipitated using an anti-UPF1 antibody, and the immunoprecipitated materials from both SILAC conditions were then combined and electrophoretically separated on an SDS-PAGE. Subsequently, the lane was cut into a dozen gel pieces (avoiding the regions of the heavy and light chain of the antibody; see Figure 1B), tryptic digestions were performed, and the resulting peptide mixtures were analyzed twice by LC−MS/MS as technical replicates. Each experiment was replicated with inversed labeling, except for the hyper-phosphorylation experiment in which the labeling was identical in the replicates. Quantification of the protein groups was calculated by MaxQuant algorithm, based on the median of the SILAC peptide ratios. The normalized ratio value was used for all calculations, except for the UPF1 competitor peptide experiment, where the unequal distribution of the ratios is inherent to the experiment (Supplementary Table S1 in the Supporting Information).

For the IPs, we used an antibody that recognizes the C-terminus of UPF1. Western blot analysis of whole HeLa cell extract (Figure 1C, lane 1) and immunoprecipitated proteins (lane 2) showed that, although recognizing additional denatured proteins (lane 1, input), the antibody does not interact with these proteins under native conditions (lane 2, IP eluate). Hence, this antibody is suitable to specifically IP endogenous UPF1 and its interactors. The faint band that was detected at ∼57 kDa most likely represents denatured IgG-binding protein G that might have detached from the beads during heat denaturation.

Discrimination between UPF1-Dependent Interactors and Unspecific Contaminants

With the first set of SILAC experiments, we wanted to identify proteins that specifically copurified with endogenous UPF1 and distinguish them from unspecific contaminants. To this end, we added to one cell lysate a 25× molar excess (relative to the anti-UPF1 antibody amount) of a peptide comprising the antibody's epitope to competitively inhibit binding of UPF1. Unspecific contaminants will copurify to a similar extent in this peptide-mediated mock IP and in the UPF1 IP, whereas UPF1-specific interactors are expected to be significantly more abundant in the UPF1 IP than in the mock IP. Confirming the efficacy of this approach, the addition of the inhibitory peptide to the heavy lysate (H) resulted in a strong reduction of UPF1 and a concomitant loss of its well-known interactors UPF2 and UPF3B in the eluate (Figure 2A, compare lanes 5 and 6). The experiment was replicated under reverse labeling conditions, and the results of both mass spectrometric analyses are shown in Figure 2B. 168 proteins have been identified in both replicates and quantified. Their protein intensities and respective H/L ratios showed a clear correlation (Supplementary Figure S2 in the Supporting Information; Figure 2B). Most of the 168 identified proteins showed a strong decrease in abundance upon the addition of the inhibitory peptide, indicating that they were immunoprecipitated in a UPF1-dependent manner. For 12 proteins, the ratio between UPF1 IP and mock IP did not change or hardly changed, suggesting that they copurified independently of UPF1 ("background proteins (not UPF1 specific)", Supplementary Table S2 in the Supporting Information). These proteins also did not change upon RNase A treatment (see later), further confirming that they most likely represent unspecific contaminants. In summary, the data obtained from the peptide competition SILAC experiments allow a clear discrimination between UPF1-dependent interactors and nonspecifically copurifying contaminants.

Discrimination between RNA-Mediated and Direct or Protein-Mediated UPF1 Interactors

Because UPF1 is an RNA-associated helicase that appears to bind mRNA independent of translation,[34] we next wanted to determine which of the 168 proteins identified in the previous experiment were simply bound to the same RNA as UPF1 and which ones associated with UPF1 directly or indirectly through protein−protein interactions. To distinguish between RNA-mediated and RNA-independent interactors, we used the SILAC approach and treated one cell lysate with RNase A (200 μg/mL final concentration) before and during the co-IP and checked the relative ratios via mass spectrometry using a nontreated cell pool as a control. The RNase A treatment resulted indeed in a clearly decreased copurification of general mRNA-binding proteins, such as the poly(A)-binding protein PABPC1 (Figure 3A, lane 6), whereas the known direct interactor UPF2 was still detected in the RNase A-treated IP (Figure 3A).

The reproducibility of the replicate experiments with reverse labeling conditions showed a Pearson correlation coefficient of −0.68, which is in the range of the biological variation within such experiments (Figure 3B). 158 proteins were identified in

dx.doi.org/10.1021/pr5002143 | J. Proteome Res. XXXX, XXX, XXX−XXX

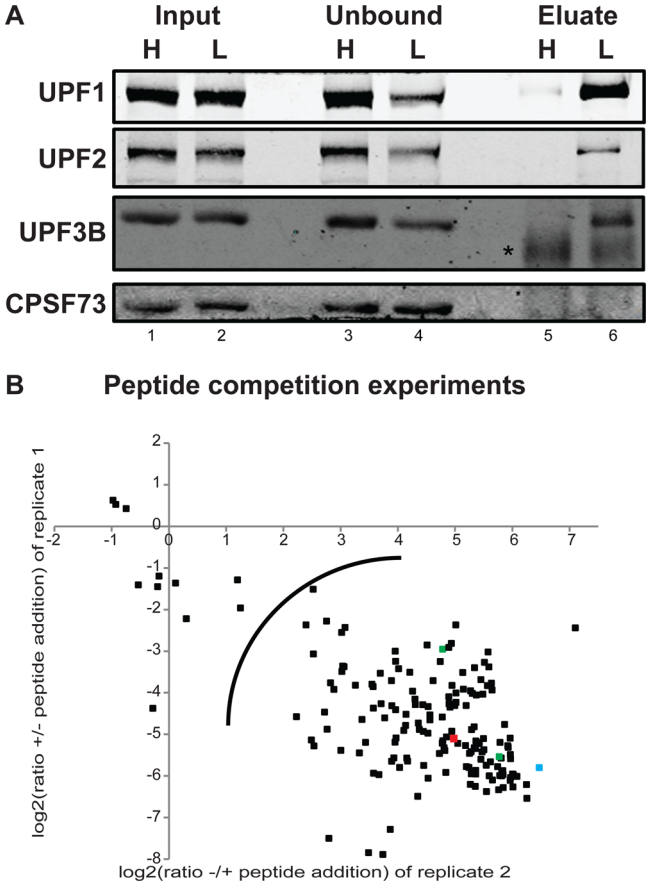

Figure 2. Discrimination between UPF1-specific interactors and unspecific contaminants by sequestration of antibody binding sites with competing peptides. (A) Addition of epitope-mimicking UPF1 peptides to the H lysate before IP abolishes precipitation of UPF1 and copurification of the UPF1 interactors UPF2 and UPF3B (compare lanes 5 and 6). CPSF73 does not interact with UPF1 and serves as specificity control. The asterisk in the UPF3B panel depicts the heavy chain of the anti-UPF1 antibody. (B) The scatter plot shows the log 2 values of the intensity ratios of two independent peptide competition experiments with inverted labeling conditions. All proteins identified in both replicates are depicted as black squares. The two isoforms of UPF1 are highlighted in green, UPF2 in red, and UPF3B in blue. The proteins in the lower right corner (right and below of the black curve) are considered to be UPF1-dependent interactors, and the others in the center are UPF1-independent contaminants. The correlation coefficient (R^2) between the replicates is −0.58.

both experiments (Supplementary Table S3 in the Supporting Information). Although the data points clearly form a cluster that remains essentially unaffected by RNase A treatment (referred to as RNA-independent interactors) and a second cluster that shows a 8−32-fold reduced copurification with UPF1 upon RNase A digestion (referred to as RNA-mediated interactors), there are also a number of proteins that reside in between these two populations and for which it is not possible to unambiguously assign them as RNA-mediated or RNA-independent (Figure 3B, dots between the two red curves, designated as "unclear RNA dependence").

A comparison between proteins measured in both RNase treatment experiments (Figure 3B) with those factors identified as UPF1-specific interactors in both replicates of the peptide competition experiment (Figure 2B) and with the proteins that were later identified in phosphorylation-dependent experiments shows a high reproducibility (Figure 3C). A set of 130 proteins was identified in all six experiments and consists of proteins that robustly and specifically coimmunopreciptated with UPF1 with a high signal-to-noise ratio, hence likely representing true UPF1 interactors, either mRNA-mediated or direct. This high overlap and consistency between the different SILAC experiments allows for a combined analysis and characterization of these 130 proteins with regard to their dependence on UPF1 and RNA. A scatter plot positioning the proteins according to their log 2 (test/control) ratios in the peptide competition (y axis) and in the RNase treatment (x axis) experiments reveals three clusters (Figure 3D): one cluster constitutes background proteins that did not change either upon addition of the UPF1 epitope-mimicking peptide or upon RNase A treatment (8 proteins; 6%). For a substantial fraction of the remaining UPF1-specific hits (70 proteins; 54%), their association with UPF1 seems to be mediated by RNA, which is expected because UPF1 is an mRNA-binding protein.[18,34,35] Among them there are the poly(A)-binding proteins and many hnRNPs, as expected. (See Supplementary Table S4 in the Supporting Information for a complete list.) The third group, consisting of 52 proteins (40%), showed no or mild RNA-dependent UPF1 association (Table 1). Confirming previous work, UPF2 and UPF3B were found in this group of protein-mediated UPF1 interactors.[36] Furthermore, the EJC components CASC3 (MLN51) and eIF4A3 have been identified, although their interaction with UPF1 seems partially RNase-A-sensitive (especially for eIF4A3, which was identified as one of those proteins with an unclear mRNA-dependence). In addition, the previously reported interaction with Staufen homologue 2 (STAU2)[37] was also identified as an mRNA-independent UPF1 interactor, while contrary to expectation, we could not detect STAU1 in our experiments.

Interestingly, among the mRNA-independent UPF1 interactors, we identified 7 (subunits a−e, i, and l) out of 13 total subunits of the eukaryotic translation initiation complex 3 (eIF3). Furthermore, subunit g was also identified in all six experiments but not always with sufficient peptide numbers to qualify as a hit, and subunits m and h were identified in 5 out of 6 experiments (Supplementary Table S5 in the Supporting Information), suggesting that UPF1 interacts with the fully assembled functional eIF3 complex. Consistently, several eIF3 subunits have previously been shown to play a role in NMD,[38−40] and based on results from far western analysis, eIF3a was proposed to be the subunit that directly binds to UPF1.[38] However, the functional consequence of the UPF1-eIF3 interaction is not yet clear. While the eIF3 subunit f was reported to inhibit NMD of mRNAs with a PTC in the first exon,[40] subunit e (also called INT6) was reported to be required for NMD.[39] Notably, eIF3f was detected in only three out of six SILAC experiments, and the obtained low signal-to-noise ratio prevented any conclusions with regard to the specificity and RNase A sensitivity of eIF3f's association with UPF1 (Supplementary Table S5 in the Supporting Information).

In addition to eIF3, several ribosomal proteins from both the 40S and the 60S ribosomal subunits appeared among the RNA-independent interactors of UPF1 (Table 1, ribosomal subunits). While overall these eight proteins (ribosomal proteins L3, L4, L5, L8, S2, S3, S3a, and S6) locate to different areas within the eukaryotic ribosome based on the X-ray structure of *Tetrahymena thermophila*,[41,42] we would like to point out that small subunit proteins S3 and S3a are positioned

dx.doi.org/10.1021/pr5002143 | J. Proteome Res. XXXX, XXX, XXX−XXX

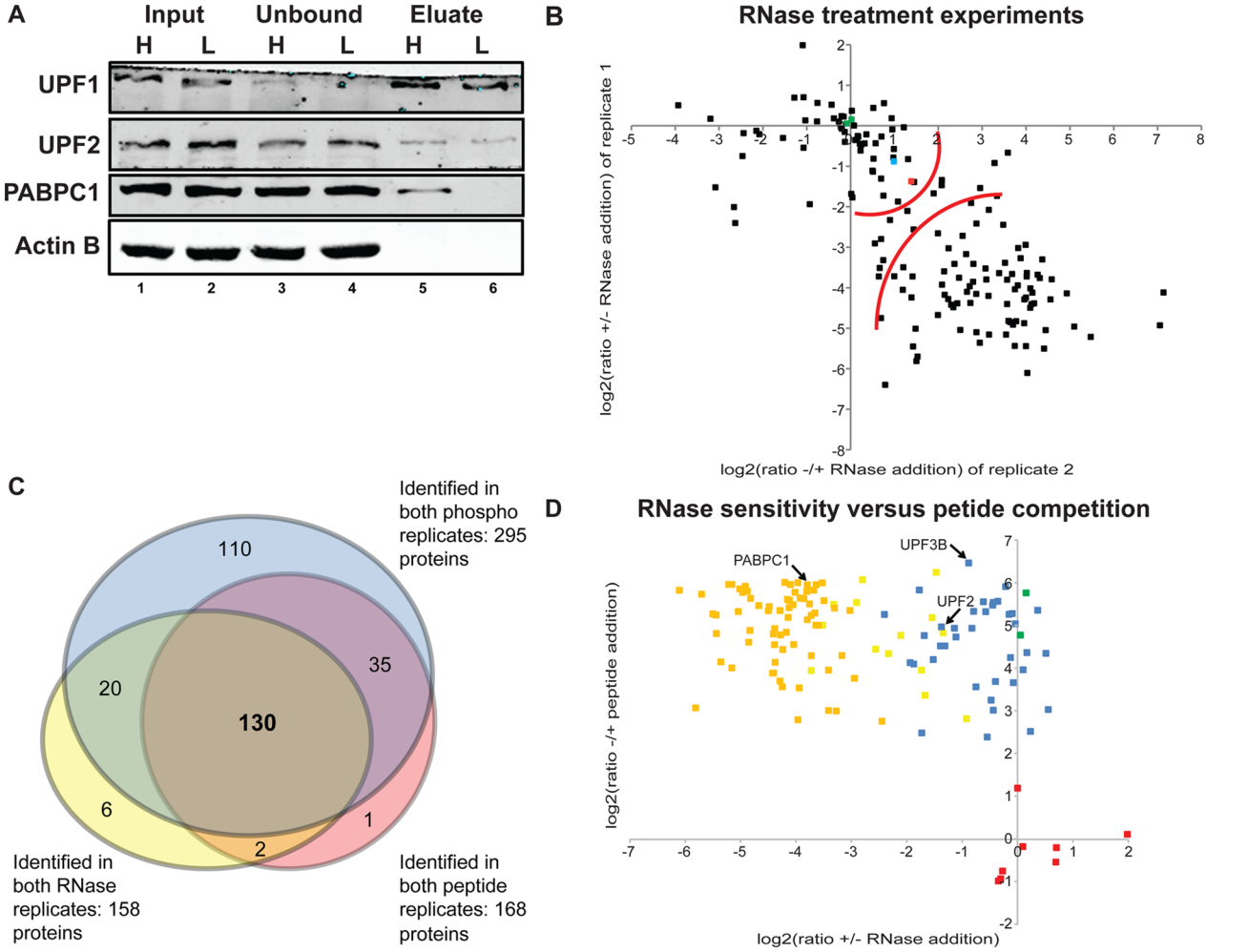

Figure 3. Discrimination between RNA-mediated and protein-mediated interactors by treatment of lysates with RNase A. (A) Western blot of inputs (lanes 1, 2), unbound material (lanes 3, 4), and eluates (lanes 5, 6) of H- and L-labeled HeLa cell lysates, of which the L lysate was incubated with RNase A prior to the IP. The known RNA-mediated association of polyA-binding protein C1 (PABPC1) was probed to check the efficiency of the RNase A treatment, whereas the direct interaction of UPF2 served as a positive control (not affected by RNase A treatment). Actin B does not associate with UPF1 and served as a negative control. (B) Correlation between RNase A-treated replicates. Log 2 values of the intensity ratios of two independent experiments with reverse labeling conditions are plotted. All proteins identified in both replicates are depicted as black squares. The two UPF1 isoforms are highlighted in green, UPF2 in red, and UPF3B in blue. R^2 between the replicates is −0.68. The red curves indicate the thresholds set for assigning a protein as RNA-independent (upper right) or RNA-mediated interactors of UPF1 (lower left). Proteins located between the two curves were categorized as "unclear RNA dependence". (C) Venn diagram displaying overlap of proteins identified in the three SILAC approaches. Red represents proteins identified as specific UPF1 interactors in both peptide competition experiments (Supplementary Table S2 in the Supporting Information), yellow depicts proteins identified in both RNase replicates (Supplementary Table S3 in the Supporting Information), and blue are proteins identified in both phospho-UPF1 replicates (Supplementary Table S6 in the Supporting Information). (D) 130 proteins identified in all three groups (panel C) were plotted according to their specificity for UPF1 (vertical axis, log 2 ratio) and their sensitivity of the UPF1 interaction to RNase A (horizontal axis, log 2 ratio). Proteins that did not change upon peptide competition or RNase A treatment are considered background (red). UPF1-specific interactors sensitive to RNase treatment are depicted in orange, RNase-resistant ones in blue, and those with unclear RNA dependence in yellow. The two isoforms of UPF1 are shown in green.

in immediate vicinity of RpS26, which has been recently shown to interact with the CH domain of Upf1p in *Saccharomyces cerevisiae*.[43]

Furthermore, our SILAC analysis identified several other RNA-independent UPF1 interactors that so far have not been linked to UPF1 (Table 1, other identified proteins) and might provide an interesting starting point for characterizing new factors involved in NMD and other UPF-dependent processes and for discovering potential new roles of UPF1 in other cellular pathways. Among these hits, there are several ATP-dependent RNA helicases, the nuclear fragile X mental retardation protein interacting protein 2 (NUFIP2, which interacts with the fragile X mental retardation protein (FMRP)[44]) and the serine-threonine kinase receptor-associated protein (STRAP, which has been implicated in SMN complex assembly and internal translation initiation; see later) to name just a few.

Phosphorylation-Dependent Interactions

The best-characterized and functionally essential posttranslational modification of UPF1 is its phosphorylation. The cycle of phosphorylation and dephosphorylation of UPF1 is essential for NMD,[9,19,45] and specific T/SQ phospho-epitopes in the N-terminus and C-terminus of UPF1 have been shown to be crucial for interaction with SMG6 and the SMG5:SMG7 heterodimer, respectively.[12] These phosphorylations are mainly

dx.doi.org/10.1021/pr5002143 | J. Proteome Res. XXXX, XXX, XXX−XXX

Table 1. Identified Proteins That Interact with UPF1 Independently of RNA or for Which the RNA Dependence of Its Interaction with UPF1 Remains Unclear (Grey)[a]

UNIPROT accession code	Protein Name	Peptide comp. #1	Peptide comp. #2	RNase treat. #1	RNase treat. #2
Nonsense-mediated mRNA decay (NMD)					
Q9HAU5	Regulator of nonsense transcripts 2	-5.11	4.98	1.39	-1.37
Q9BZI7	Regulator of nonsense transcripts 3B	-5.80	6.47	0.99	-0.88
O15234	Protein CASC3 (MLN51)	-6.06	4.53	1.45	-1.39
P38919	Eukaryotic initiation factor 4A-III	-6.54	6.25	2.08	-1.47
Eukaryotic initiation factor 3 subunits (eIF3)					
Q14152	Eukaryotic translation initiation factor 3 subunit A	-3.25	4.74	0.50	-1.11
P55884	Eukaryotic translation initiation factor 3 subunit B	-3.82	4.94	0.51	-1.14
Q99613	Eukaryotic translation initiation factor 3 subunit C	-4.82	5.33	0.99	-0.57
O15371	Eukaryotic translation initiation factor 3 subunit D	-3.83	5.57	0.23	-0.62
P60228	Eukaryotic translation initiation factor 3 subunit E	-4.04	5.49	0.21	-0.45
Q13347	Eukaryotic translation initiation factor 3 subunit I	-6.37	5.55	0.32	-0.44
Q9Y262	Eukaryotic translation initiation factor 3 subunit L	-3.02	5.58	0.11	-0.36
Ribosomal proteins					
P23396	40S ribosomal protein S3	-5.21	4.77	0.02	-1.68
P61247	40S ribosomal protein S3a	-5.75	5.55	0.56	-2.91
P62753	40S ribosomal protein S6	-5.22	5.05	1.22	-0.04
P15880	40S ribosomal protein S2	-6.20	5.27	-2.63	-2.40
P39023	60S ribosomal protein L3	-4.33	4.53	0.70	-1.31
P36578	60S ribosomal protein L4	-6.49	4.35	0.90	-2.33
P46777	60S ribosomal protein L5	-4.37	3.57	-2.46	-0.75
P62917	60S ribosomal protein L8	-4.79	4.14	-0.93	-1.94
Other identified proteins					
Q99700	Ataxin-2	-4.31	5.19	2.96	-1.54
Q08211	ATP-dependent RNA helicase A	-3.76	2.82	3.29	-0.92
Q92499	ATP-dependent RNA helicase DDX1	-6.28	5.84	0.04	-1.77
O00571	ATP-dependent RNA helicase DDX3X	-5.37	5.50	0.75	-3.32
P60842	ATP-dependent RNA helicase eIF4A-1	-4.91	4.10	1.09	-1.87
Q53EZ4	Centrosomal protein of 55 kDa	-5.97	3.67	-0.20	-0.08
Q96EY1	DnaJ homolog subfamily A member 3, mitochondrial	-4.64	3.37	1.90	-1.67
Q9H223	EH domain-containing protein 4	-5.09	3.97	-0.76	0.10
P08107	Heat shock 70 kDa protein 1A/1B	-3.82	3.26	0.24	-0.48
P11142	Heat shock cognate 71 kDa protein	-3.49	3.02	0.57	-0.44
P10809	60 kDa heat shock protein, mitochondrial	-3.36	3.04	0.76	0.56
P11021	78 kDa glucose-regulated protein	-2.37	2.40	-1.07	-0.55
O75569	Interferon-inducible double stranded RNA-dependent protein kinase activator A	-3.40	5.34	0.98	-0.79
Q92615	La-related protein 4B	-4.23	5.01	0.66	-3.51
Q09161	Nuclear cap-binding protein subunit 1 (CBP80)	-3.00	3.95	0.65	-3.72
Q7Z417	Nuclear fragile X mental retardation-interacting protein2	-6.01	6.08	0.70	-2.80
Q8NCA5	Protein FAM98A	-4.93	4.94	1.32	-0.82

dx.doi.org/10.1021/pr5002143 | J. Proteome Res. XXXX, XXX, XXX−XXX

Table 1. continued

UNIPROT accession code	Protein Name	Peptide comp. #1	Peptide comp. #2	RNase treat. #1	RNase treat. #2
Other identified proteins					
Q96T37	Putative RNA-binding protein 15	-3.96	4.26	-2.14	-0.13
Q86TG7	Retrotransposon-derived protein PEG10	-5.75	4.45	1.44	-2.56
Q52LW3	Rho GTPase-activating protein 29	-3.53	3.69	-0.13	-0.40
Q96PK6	RNA-binding protein 14	-3.51	4.21	-3.08	-1.52
O94806	Serine/threonine-protein kinase D3	-5.27	5.92	0.36	-0.21
Q9Y3F4	Serine-threonine kinase receptor-associated protein (UNR-interacting protein)	-5.16	5.36	0.03	0.37
P55011	Solute carrier family 12 member 2	-3.95	5.27	-0.13	-0.15
O94864	STAGA complex 65 subunit gamma	-4.88	4.37	-3.19	0.17
Q9NUL3	Double-stranded RNA-binding protein Staufen 2	-4.89	5.29	0.96	-0.09
P49368	T-complex protein 1 subunit gamma	-3.07	2.52	-0.20	0.23
Q16881	Thioredoxin reductase 1, cytoplasmic	-4.73	4.36	-0.43	0.51
Q9Y3I0	tRNA-splicing ligase RtcB homolog	-5.91	4.84	2.08	-1.34
Q9H7E2	Tudor domain-containing protein 3	-4.59	4.78	1.30	-2.11
Q5T6F2	Ubiquitin-associated protein 2	-5.14	2.49	0.75	-1.73

[a]Depicted are the H/L ratios (log 2 scale) of the peptide competition experiments #1 and #2 and of the RNase A-treatment experiments #1 and #2. Peptide was added to sample H in the petide competition experiment #1 and to sample L in experiment #2. RNase A was added to sample L in the RNase-treatment experiment #1 and to sample H in experiment #2.

mediated by the phosphatidylinositol 3-kinase-related kinase (PIKK) SMG1. Given the important role of phosphorylation for UPF1 function, we decided to apply the SILAC approach to identify and compare interactors of the hyper- and of the hypo-phosphorylated state of UPF1. Because there is only a small fraction of hyper-phosphorylated UPF1 in normally growing cells and SMG1 activity was reported to be rate-limiting for NMD,[46] we boosted the amount of phosphorylated UPF1 (pUPF1) by plasmid-based overexpression of Flag-tagged SMG1 and by treating the cells with the phosphatase 2A inhibitor okadaic acid (OA).

Treatment of the cells with OA alone for 4 h (50 nM final concentration) before harvesting resulted only in a moderate up-regulation compared with untreated cells (Supplementary Figure S3 in the Supporting Information). However, additional two-fold overexpression of Flag-SMG1 (Figure 4A) resulted in a robust 20-fold increase in UPF1 phosphorylation (pUPF1/UPF1 ratio; Figure 4B). As a negative control, Flag-GFP was expressed in the heavy samples. Two biologically independent replicates of this experiment were performed, and both times SMG1 was overexpressed in the L cells followed by OA treatment. MS analysis of the samples identified a set of 295 proteins with a high reproducibility (Figure 4C, see Supplementary Table S6 in the Supporting Information for a complete list), of which several proteins showed a clear preference for hyper- or hypo-phosphorylated UPF1 (>1.5-fold change between hyper-phosphorylation and control conditions in both replicates), emphasizing the impact of this post-translational modification on UPF1 function (summarized in Table 2). Because 110 of the proteins interacting preferentially with pUPF1 were not detected in the other experiments due to their low abundance in the immunoprecipitates as a result of the low abundance of pUPF1 in normally grown cells, we did not restrict our analysis on the set of 130 commonly identified proteins (see previous) but instead included all 295 proteins identified in both phospho-SILAC replicate experiments.

Of the three NMD factors that were previously shown to preferentially bind to pUPF1 (SMG5, SMG6, and SMG7),[12] only SMG5 and SMG7 could be detected reproducibly in our SILAC experiments. The low abundance in HeLa cells, inefficient ionization of its peptides, or the masking of weak interaction surfaces by the antibody used for IP are possible reasons for the failure to detect SMG6 in the UPF1 IPs. While SMG7 displayed no strong preference for pUPF1, SMG5 indeed showed a preferential association with pUPF1 (Table 2 and Figure 4C).

Interestingly and unexpectedly in the light that only a minor fraction of the cellular UPF1 localizes to the nucleus,[36] gene ontology (GO) analysis[47] revealed a significant enrichment among the proteins that preferentially copurified with pUPF1 for GO terms describing nuclear functions such as pre-mRNA splicing and mRNA export (Figure 4D). Noteworthy, all six described human THO complex subunits,[48] including the associated RNA-binding export factor THOC4 (ALY/REF), were identified to interact with pUPF1 (Figure 4C) but were not detected in experiments where the cells were not treated with OA, suggesting a phosphorylation-specific association of UPF1 with the transcription-export (TREX) complex, which was previously shown to be recruited to mRNA during splicing[48] and to promote mRNA export.[49,50]

Also, the two EJC components CASC3 (MLN51; identified as an RNA-independent UPF1 interactor) and eIF4AIII (unclear RNA-dependence; Table 1), revealed a significant preference for pUPF1 (Figure 4C and Table 2). Similar to TREX, the EJC also assembles on mRNA during splicing,[51−53] implying that pUPF1 might also bind to mRNA during or after splicing inside the nucleus. (See the Discussion.) In addition, several hnRNPs (A/B, A1, A2/B1, A3, D0, H3, L, and R), the mRNA export receptor TAP/NXF1, the U5 snRNP

dx.doi.org/10.1021/pr5002143 | J. Proteome Res. XXXX, XXX, XXX−XXX

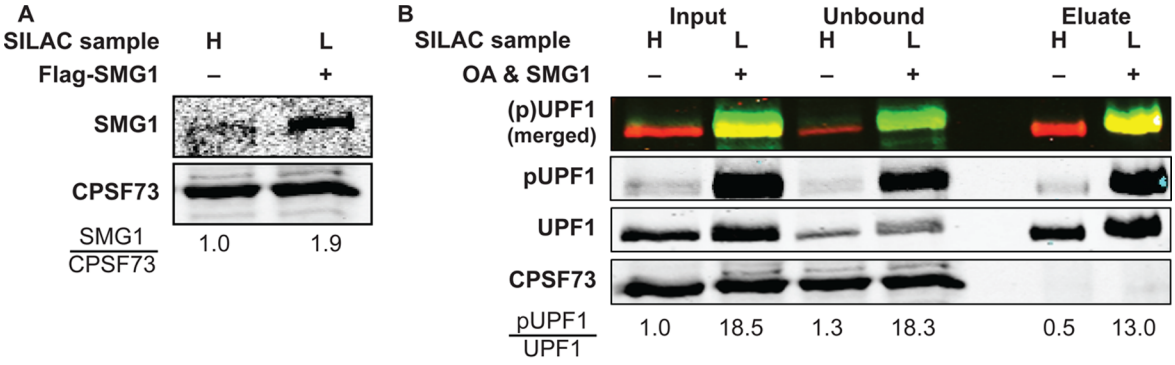

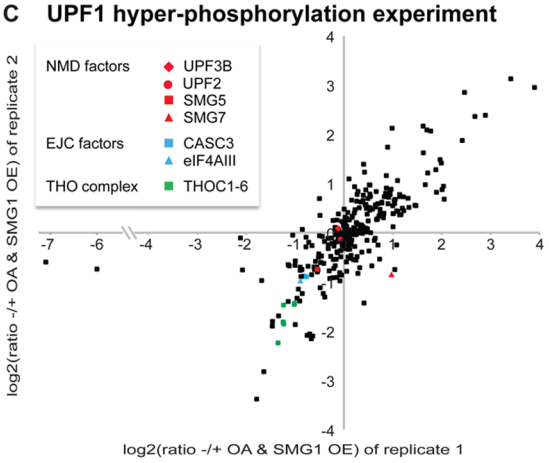

D GO analysis

	GO Term	P-value	# of proteins
>1.5fold up in hyperpUPF1	TRANSCRIPTION EXPORT COMPLEX	2.25E-11	6 (43)
	INTRONLESS VIRAL MRNA EXPORT FROM HOST NUCLEUS	2.25E-11	6 (43)
	MRNA EXPORT FROM NUCLEUS	8.05E-09	7 (43)
	HETEROGENEOUS NUCLEAR RIBONUCLEOPROTEIN COMPLEX	9.69E-09	6 (43)
	RIBONUCLEOPROTEIN COMPLEX	2.31E-08	8 (43)
	RNA SPLICING	4.30E-08	10 (43)
	RNA BINDING	1.27E-04	8 (43)
	PROTEIN BINDING	0.01	32 (43)
	NUCLEOLUS	0.01	9 (43)
	NUCLEUS	0.01	15 (43)
>1.5fold down in hyper pUPF1	***CYTOSOL***	0.01	14 (45)
	PROTEIN BINDING	0.01	27 (45)
	CYTOPLASM	0.07	12 (45)

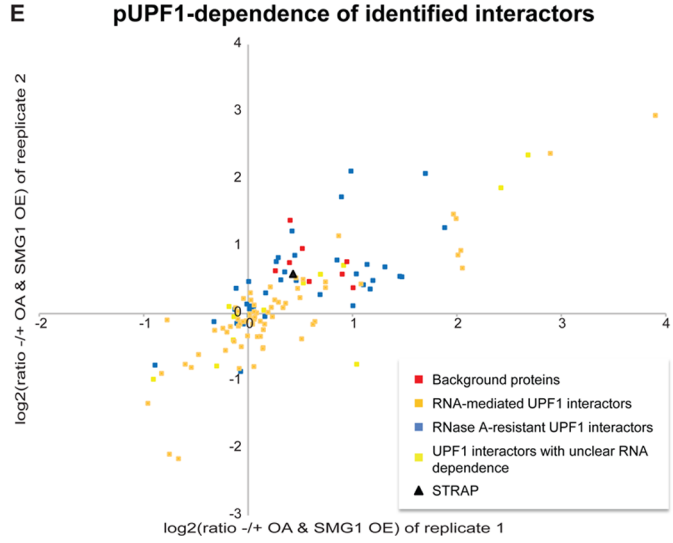

Figure 4. Differential interaction of proteins with hyper- or hypo-phosphorylated UPF1. (A) Immunoblot documenting the overexpression of SMG1. Flag-SMG1 encoding plasmid was transfected in the L cells, whereas H cells received the empty Flag-encoding plasmid as a control. 44 h post transfection, cells were lysed and SMG1 levels were detected by Western blotting using anti-SMG1 antibody. Detection of CPSF73 served as loading control. (B) Immunoblot showing the IP of predominantly phosphorylated UPF1 upon okadaic acid (OA) treatment and SMG1 overexpression. The Flag-SMG1 expressing L cells were treated with OA for 4 h prior to harvesting. UPF1 was detected with anti-UPF1 antibody (red in upper panel), and phosphorylated UPF1 (pUPF1) was detected by a antiphospho(S/T)Q-specific antibody (green in upper panel). CPSF73 does not interact with UPF1 and served as IP specificity control. (C) Scatter plot showing the log 2 values of the intensity ratios of two independent phospho-UPF1 experiments. R^2 between the replicates is 0.60. Negative ratios represent preferential interaction with pUPF1 (lower left corner), and positive ratios represent preferential interaction with hypo-phosphorylated UPF1 (upper right corner). The NMD factors UPF2, UPF3B, SMG5, and SMG7, the EJC factors CASC3/MLN51 and eIF4AIII, and the 6 THO complex subunits are highlighted. (D) GO annotation table[47] based on UPF1 interactors with a preference for hyper- or hypo-phosphorylated UPF1 (intensity ratios change of >1.5-fold). *P* values and the number of proteins in the respective GO category are indicated. All 43 proteins with a preference for pUPF1 and all 45 proteins with a preference for hypo-phosphorylated UPF1 were included in the GO annotation analysis. (E) Scatter plot as in panel C but restricted to the 130 proteins identified in all experiments. (See Figure 3C.) Proteins were categorized and displayed as in Figure 3D; STRAP is denoted as black triangle.

dx.doi.org/10.1021/pr5002143 | *J. Proteome Res.* XXXX, XXX, XXX−XXX

Table 2. List of Proteins with a Phosphorylation State-Dependent Differential UPF1 Association[a]

log2 (OA+SMG1/control)		Uniprot ID	Protein names
Exp.1	Exp.2		
-1.64	-2.83	P46013	Antigen KI-67
-0.99	-0.58	Q9NVI7	ATPase family AAA domain-containing protein 3A
-1.14	-0.65	Q5T9A4	ATPase family AAA domain-containing protein 3B
-1.78	-3.38	P28288	ATP-binding cassette sub-family D member 3
-0.55	-0.70	P07814	Bifunctional glutamate/proline--tRNA ligase
-1.34	-1.69	Q7Z7K6	Centromere protein V
-1.00	-0.67	Q9Y3Y2	Chromatin target of PRMT1 protein
-1.47	-1.90	P20908	Collagen alpha-1(V) chain
-7.17	-0.58	P78527	DNA-dependent protein kinase catalytic subunit
-6.11	-0.74	O95714	E3 ubiquitin-protein ligase HERC2
-0.91	-0.98	P38919	Eukaryotic initiation factor 4A-III
-0.77	-0.90	Q99729	Heterogeneous nuclear ribonucleoprotein A/B
-1.14	-1.40	P09651	Heterogeneous nuclear ribonucleoprotein A1
-0.66	-0.86	P51991	Heterogeneous nuclear ribonucleoprotein A3
-0.60	-0.75	Q14103	Heterogeneous nuclear ribonucleoprotein D0
-0.61	-0.70	P31942	Heterogeneous nuclear ribonucleoprotein H3
-0.90	-1.39	P14866	Heterogeneous nuclear ribonucleoprotein L
-0.73	-0.68	O43390	Heterogeneous nuclear ribonucleoprotein R
-0.83	-0.89	P22626	Heterogeneous nuclear ribonucleoproteins A2/B1
-1.00	-1.87	P48200	Iron-responsive element-binding protein 2
-0.86	-0.75	O43896	Kinesin-like protein KIF1C
-0.85	-1.24	P42704	Leucine-rich PPR motif-containing protein, mitochondrial
-0.75	-2.09	Q15233	Non-POU domain-containing octamer-binding protein
-1.12	-0.68	Q9UBU9	Nuclear RNA export factor 1
-1.46	-1.80	Q9NR30	Nucleolar RNA helicase 2
-0.58	-0.59	P06748	Nucleophosmin
-0.64	-2.10	Q6P2Q9	Pre-mRNA-processing-splicing factor 8 (PRPF8)
-0.89	-0.70	Q02809	Procollagen-lysine,2-oxoglutarate 5-dioxygenase 1
-0.89	-0.77	O15234	Protein CASC3
-0.96	-1.33	Q9P2E9	Ribosome-binding protein 1
-2.08	-0.76	P22087	rRNA 2-O-methyltransferase fibrillarin
-0.88	-0.89	P36873	Serine/threonine-protein phosphatase PP1-gamma catalytic subunit
-0.67	-2.16	P23246	Splicing factor, proline- and glutamine-rich (SFPQ)
-0.93	-1.15	O95425	Supervillin
-1.24	-1.47	Q96FV9	THO complex subunit 1
-1.23	-1.86	Q8NI27	THO complex subunit 2
-1.01	-1.44	Q96J01	THO complex subunit 3
-1.35	-2.24	Q86V81	THO complex subunit 4
-1.24	-1.82	Q13769	THO complex subunit 5 homolog
-1.02	-1.46	Q86W42	THO complex subunit 6 homolog
-0.70	-2.06	O75643	U5 small nuclear ribonucleoprotein 200 kDa helicase (SNRNP200)
-0.90	-0.77	A4D1P6	WD repeat-containing protein 91
-1.68	-0.97	Q96KR1	Zinc finger RNA-binding protein
0.97	0.88	P61981	14-3-3 protein gamma
0.89	1.74	P10809	60 kDa heat shock protein, mitochondrial
0.90	0.59	P06733	Alpha-enolase
2.04	0.94	O95782	AP-2 complex subunit alpha-1
1.89	0.82	O94973	AP-2 complex subunit alpha-2
2.05	0.68	P63010	AP-2 complex subunit beta
2.01	0.87	Q96CW1	AP-2 complex subunit mu
2.68	2.36	Q99700	Ataxin-2
0.92	0.72	O00571	ATP-dependent RNA helicase DDX3X
0.66	0.83	P31327	Carbamoyl-phosphate synthase [ammonia], mitochondrial
0.83	0.73	Q96EP5	DAZ-associated protein 1
0.65	0.56	Q8WXX5	DnaJ homolog subfamily C member 9
1.31	0.70	P60842	Eukaryotic initiation factor 4A-I
1.04	0.59	O15371	Eukaryotic translation initiation factor 3 subunit D
1.14	0.73	Q13347	Eukaryotic translation initiation factor 3 subunit I
1.72	1.21	O43432	Eukaryotic translation initiation factor 4 gamma 3
1.62	2.16	P15311	Ezrin
1.05	0.68	Q14315	Filamin-C
2.90	2.38	P51114	Fragile X mental retardation syndrome-related protein 1
1.97	1.48	P51116	Fragile X mental retardation syndrome-related protein 2
0.95	0.77	P04406	Glyceraldehyde-3-phosphate dehydrogenase
0.90	0.58	P63244	Guanine nucleotide-binding protein subunit beta-2-like 1
0.94	0.84	P07900	Heat shock protein HSP 90-alpha
0.78	0.60	P08238	Heat shock protein HSP 90-beta
2.42	1.87	Q92615	La-related protein 4B
1.22	0.73	P07195	L-lactate dehydrogenase B chain
0.69	0.59	Q09161	Nuclear cap-binding protein subunit 1

dx.doi.org/10.1021/pr5002143 | J. Proteome Res. XXXX, XXX, XXX−XXX

Table 2. continued

log2 (OA+SMG1/control)		Uniprot ID	Protein names
Exp.1	Exp.2		
1.03	0.66	Q15149	Plectin
0.87	1.16	Q9H0J9	Poly [ADP-ribose] polymerase 12
1.63	1.62	Q9H6S0	Probable ATP-dependent RNA helicase YTHDC2
0.78	0.62	Q99873	Protein arginine N-methyltransferase 1
1.78	2.06	Q5JSZ5	Protein PRRC2B
3.90	2.95	Q15032	R3H domain-containing protein 1
1.88	1.28	Q52LW3	Rho GTPase-activating protein 29
3.41	3.12	Q8IXT5	RNA-binding motif protein 12B
1.14	0.77	Q16629	Serine/arginine-rich splicing factor 7
1.70	2.09	O94806	Serine/threonine-protein kinase D3
1.67	0.97	Q9BXP5	Serrate RNA effector molecule homolog
1.45	0.56	P55011	Solute carrier family 12 member 2
0.99	2.12	O94864	STAGA complex 65 subunit gamma
0.87	0.90	Q92804	TATA-binding protein-associated factor 2N
1.10	1.06	P62995	Transformer-2 protein homolog beta
2.47	2.85	Q8N9M5	Transmembrane protein 102
0.85	0.80	Q5T6F2	Ubiquitin-associated protein 2
1.99	1.41	Q8IWR0	Zinc finger CCCH domain-containing protein 7A

[a]Proteins co-immunoprecipitating preferentially with hyper-phosphorylated UPF1 are indicated in orange (criteria: >1.5-fold more abundant in p-UPF1 than control sample in both SILAC replicates, 43 proteins). The proteins with a preferential association with hypo-phosphorylated UPF1 are indicated in grey (criteria: >1.5-fold less abundant in p-UPF1 than control sample in both SILAC replicates, 45 proteins).

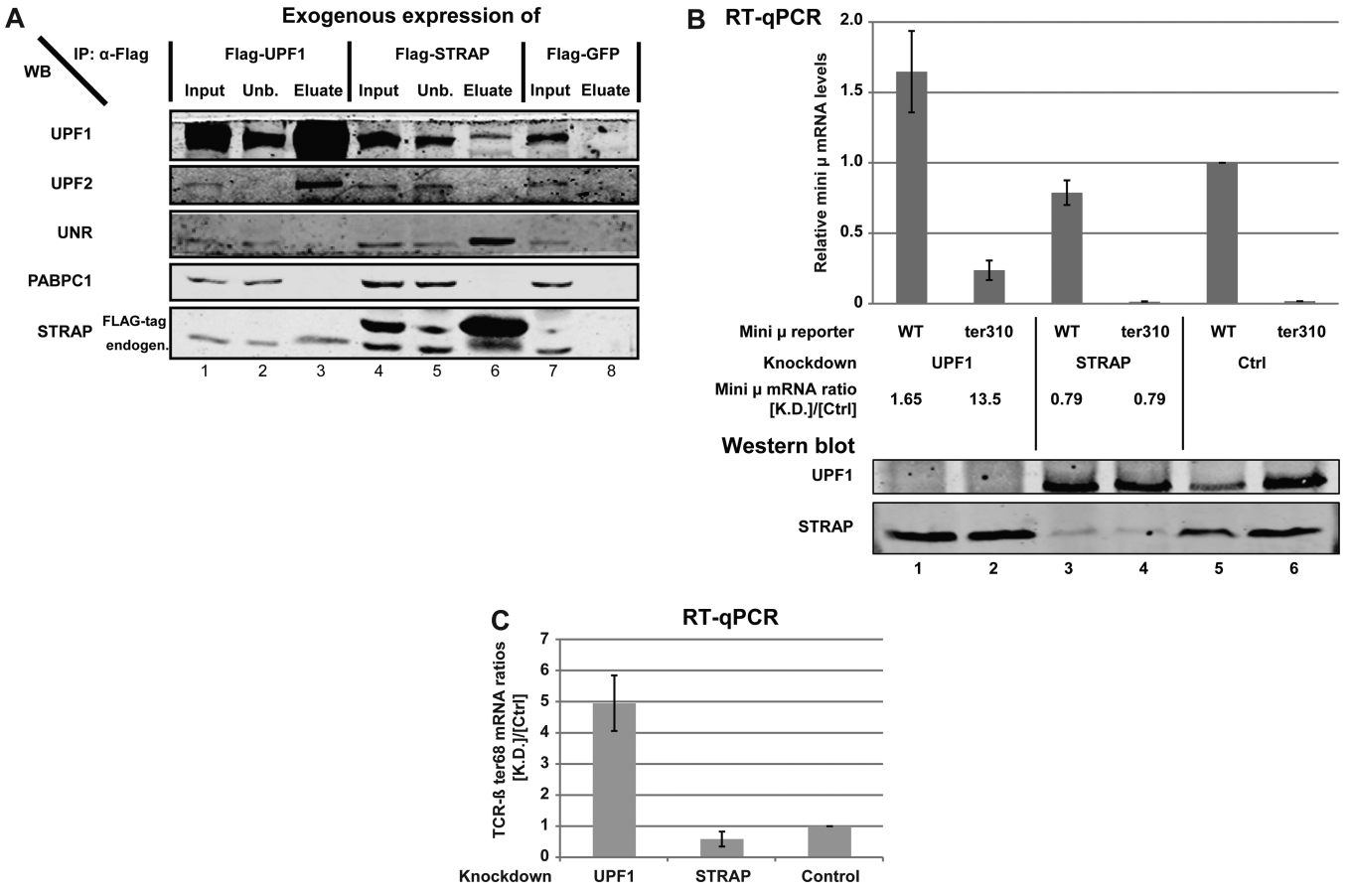

Figure 5. UPF1 interactor STRAP is not involved in NMD. (A) Immunoblot showing the interaction of Flag-tagged STRAP with endogenous UPF1 and vice versa. Plasmids encoding Flag-tagged UPF1, STRAP, or GFP (specificity control) were transfected into HeLa cells, followed by IP with anti-Flag antibody. Endogenous STRAP and UPF2, but not UNR, coprecipitated with FLAG-UPF1 (lane 3), whereas endogenous UPF1 and UNR, but not UPF2, were detected in the Flag-STRAP IP (lane 6). Loss of the RNA-mediated interactor PABPC1 in the IPs confirmed that the RNase treatment was effective. None of the tested proteins were detected in the control IP with Flag-GFP (lane 8). (B) Relative mRNA levels of the NMD reporter miniμ ter310 (PTC at position 310) and its PTC-free version (WT) in cells subjected to knockdown of UPF1 or STRAP or a control knockdown (Ctrl) are shown. RT-qPCR was performed as described in the Materials and Methods, and miniμ levels were normalized to the average levels of 18S rRNA and 7SL RNA. Average values from two independent experiments are shown. Anti-STRAP and anti-UPF1 antibodies were used to monitor STRAP and UPF1 knockdown efficiencies (Western blot; bottom panel). (C) Knockdowns were performed as in panel B with HeLa cells stably expressing the NMD reporter gene TCR β ter68. Relative TCR β mRNA levels, normalized to 18S rRNA, were determined under UPF1, STRAP, and control (Ctrl) knockdown conditions using RT-qPCR. Average values from two independent experiments are shown.

dx.doi.org/10.1021/pr5002143 | J. Proteome Res. XXXX, XXX, XXX−XXX

components PRPF8 and SNRNP200, and the PTB-associated splicing factor SFPQ also exhibited a preferential association with pUPF1. The GO term analysis of the proteins that exhibited a preference for hypo-phosphorylated UPF1 revealed a slight enrichment of the terms "cytosol" and "cytoplasm" (Figure 4D), altogether suggesting that the nuclear fraction of UPF1 might be predominantly hyper-phosphorylated, whereas the cytoplasmic UPF1 fraction would be mainly hypo-phosphorylated.

When the color code for RNase-resistant versus RNase-sensitive UPF1 interactors was applied to the scatter plot depicting phosphorylation status-dependent UPF1 interactions (Figure 4E), we noted that most proteins that were identified as protein-mediated interactors do bind UPF1 independently of its phosphorylation status or show a slight preference for hypo-phosphorylated UPF1 (blue squares), whereas the majority of the proteins with a preference for pUPF1 interact with UPF1 in a RNA-mediated manner (yellow squares), suggesting a preferred association of pUPF1 with RNA.

Verification of UPF1:STRAP Interaction

Among the many newly identified UPF1 interactors, we chose to have a closer look at the protein STRAP (serine/threonine kinase receptor-associated protein). STRAP has been reported to be involved in TGF-β signaling[54] and to assemble with the SMN complex, which is essential for the maturation of spliceosomal snRNPs.[55] By its interaction with the SMN complex component Gemin7, STRAP appears to contribute to the cytoplasmic localization of a fraction of the SMN complex.[55] In addition, STRAP has also been shown to interact with UNR (hence its second name: UNR-interacting protein, UNRIP) and in this configuration to regulate internal translation initiation of human rhinovirus RNA.[56] STRAP was detected in all experiments, it exhibited clear UPF1-specificity, did not decrease upon RNase A treatment (Table 1), and did not change much upon UPF1 hyper-phosphorylation induced by OA treatment and SMG1 overexpression (Figure 4E, black triangle).

To confirm the interaction between UPF1 and STRAP, HeLa cells were transfected with FLAG-tagged STRAP, UPF1, or GFP, respectively. Using anti-FLAG matrix, the FLAG-tagged proteins were immunoprecipitated, and the eluates were checked for the presence of several NMD-related factors by Western blotting analysis (Figure 5A). The IPs were treated with RNase A, and the loss of the mRNA-mediated interaction between FLAG-UPF1 and PABPC1 indicated efficient RNA digestion (Figure 5A, lanes 3 and 6). As anticipated by the MS results, UPF1 coimmunoprecipitated with FLAG-tagged STRAP and also the previously reported interaction with UNR could be confirmed (Figure 5A, lane 6). In addition, FLAG-tagged STRAP coimmunoprecipitated endogenous STRAP, suggesting that STRAP forms multimers in vivo. Notably, no UPF2 could be detected in the eluate fraction of FLAG-STRAP, suggesting that STRAP is not part of the UPF1:UPF2:UPF3B NMD complex.[36] Vice versa, in the eluate of the FLAG-UPF1 IP, we detected STRAP and UPF2 but not UNR. This suggests that UNR is not part of the STRAP-UPF1 complex and that hence UPF1 may not be involved in UNR-mediated translation initiation.

Despite the counter-indication from the co-IPs, we asked if STRAP might play a role in NMD. To this end, we depleted HeLa cells of STRAP or of UPF1 as a positive control by expression of the respective short hairpin (sh)RNAs. As shown by the Western blot (Figure 5B, bottom panel), knockdown of STRAP and UPF1 resulted in efficient depletion of the respective proteins in cells that expressed either a NMD reporter transcript (ter310) or the corresponding PTC-free control transcript (WT). The relative mRNA levels of these miniμ reporter transcripts were measured by RT-qPCR (Figure 5B, upper panel). Whereas the ratio between the PTC-containing miniμ ter310 construct and the miniμ wild-type construct was at ~2% (i.e., a 50-fold reduction of the PTC-containing construct due to NMD), this ratio increased to 15% upon depletion of the essential NMD factor UPF1. Under STRAP knockdown conditions, the ratio remained at 2%. To confirm this result, we also tested another NMD substrate, a PTC-containing TCR β ter68 minigene. Its levels were also unaffected by a STRAP knockdown, whereas under UPF1 knockdown conditions, the NMD substrate was stabilized five-fold (Figure 5C). The results strongly suggest that STRAP has no role in NMD, consistent with its lacking interactions with other NMD factors (Figure 5A). Thus, the biological function of the UPF1:STRAP interaction remains to be elucidated in the future.

DISCUSSION

We document here how SILAC can be used to interrogate different "states" of a protein of interest and how this can provide very detailed and specific information regarding the protein's interaction partners. Specifically, our goal was to determine the proteins associated with the key NMD factor UPF1, an ATP-dependent RNA helicase phosphoprotein. Instead of overexpressing recombinant UPF1 with an affinity tag, which would have facilitated affinity purification but would have been prone to identification of false positive interactors, we immunoprecipitated the endogenous UPF1 using a specific antibody for which the epitope on UPF1 was known. This allowed us to distinguish UPF1-specific interactors from unspecifically copurifying proteins by quenching the UPF1-IP with an excess of epitope peptide (Figure 2). The UPF1-specific interactors were subsequently separated in RNA-mediated and RNase-insensitive (i.e., most likely protein-mediated) proteins by a second set of SILAC experiments (Figure 3). Finally, in a third set of SILAC experiments, we treated one cell pool with OA and overexpressed SMG1 to increase the fraction of pUPF1, allowing the identification of interaction partners that have a preference for hyper- or hypo-phosphorylated UPF1 (Figure 4). Besides previously known interactors, we identified several dozens of new UPF1 interactors, which constitute a treasure chest for future functional studies. The information regarding RNA and phosphorylation dependence of their interaction with UPF1 provides a valuable starting point for hypothesis-driven functional studies.

Because UPF1 is an mRNA-binding enzyme, distinction between protein-mediated interactions and mRNP components that associated with UPF1 bridged by mRNA was a central task of our study and the rationale for experiments in which one of the SILAC samples was incubated with RNase A during the IP. The observed reduction upon RNase A by 10−30-fold of hnRNPs and PABPs confirmed the efficacy of the RNA digestion (Supplementary Table S3 in the Supporting Information). Detection of the well-characterized NMD factors UPF2 and UPF3b as RNA-independent UPF1 interactors further corroborated the validity of our experimental approach. We also readily detected SMG5 and found that it was 1.5- to

dx.doi.org/10.1021/pr5002143 | J. Proteome Res. XXXX, XXX, XXX−XXX

1.8-fold more abundant in the IPs of pUPF1, consistent with the previously reported preference for pUPF1.[11,12] SMG5 forms a heterodimer with the structurally related SMG7,[15] which we also identified in our experiments as a UPF1 interactor, albeit with no pronounced preference for pUPF1. In contrast, we failed to detect SMG6, which has been reported to bind via its 14−3−3 domain to UPF1 phosphorylated at T28[12] but which has been notoriously difficult to detect in IP experiments due to its low abundance.

While most detected proteins could be unambiguously categorized either as "RNA-mediated" or as "RNA-independent", there was a small fraction in between these two clusters that we termed "unclear RNA dependence" (Table 1 and Figure 3B). The main reason for not being able to assign these proteins was variations between the two replicas. A prominent factor that fell into this category is the nuclear cap-binding protein subunit 1 (CBP80), which is maybe symptomatic given the controversial data in the literature regarding its interaction with UPF1. While initially the helicase domain of UPF1 was shown to directly interact with CBP80,[57,58] a finding that served as a main pillar for a model postulating the restriction of NMD to CBC-bound mRNA,[59] we and others found the UPF1:CBP80 interaction to be RNA-mediated[12,60] and provided independent evidence of NMD of eIF4E-bound mRNA in human cells.[60,61]

Among the RNA-independent UPF1 interactors, there were many subunits of the eIF3 complex (Table 1). The eIF3 complex can be subdivided into three modules:[62] eIF3a forms together with subunits b, g, and i one module, of which in addition to a also b (Prt1p in yeast) and g have been reported to be required for NMD.[63,64] In addition, also subunit e of the module c:d:e:k:l is needed for NMD in mammalian cells,[39,40] whereas subunits f and h of module f:h:m exert the opposite effect on AUG-proximal termination codons in β-globin mRNA: they are required for the suppression of NMD at these early stops.[40] Seven of the totally 13 known eIF3 subunits (a−e, i, and l) were detected in all 6 SILAC experiments with at least two peptides (our criteria for qualifying as high confidence interactors), an additional subunit (g) was also identified in all 6 experiments but not always with 2 peptides, and subunits m and h were detected in 5 of the 6 experiments. Altogether, our data suggest an interaction of UPF1 with either the entire eIF3 complex or at least with the two eIF3 modules a:b:g:i and c:d:e:k:l. Interestingly, subunits of these two modules were found to be required for NMD,[39,40,63,64] whereas subunits f and h of the third module inhibited NMD, leading us to speculate that UPF1 might form a complex with modules a:b:g:i and c:d:e:k:l that is mutually exclusive with the interaction between module f:h:m and the other two eIF3 modules.

There is evidence that eIF3a, the largest subunit, directly interacts with UPF1 and that the interaction of pUPF1 with eIF3 impairs the eIF3-dependent translation initiation, leading to translational repression of the targeted mRNA.[38] In contrast with this study, we did not observe a preferential interaction of eIF3 with pUPF1. On the contrary, most eIF3 subunits did not show a significant difference between the hypo- and the hyper-phosphorylated UPF1 samples, and subunits d and i were even slightly (1.5- to 2-fold) reduced in the pUPF1 samples (Table 2). A possible explanation for this discrepancy could be that Isken and colleagues achieved accumulation of pUPF1 by mutating two amino acids within the ATPase/RNA helicase domain of UPF1 (positions 495 and 497), whereas we increased the pUPF1 fraction by a combination of SMG1 overexpression and OA treatment.

Among the newly identified UPF1-interacting proteins in this study, we were particularly interested in the UNR-interacting protein STRAP, which has been implicated in the regulation of internal translation initiation[56] and of the stability of *c-fos* mRNA.[65] Because UPF1 functions are also linked to translation and mRNA stability, we hypothesized that the RNase-resistant physical interaction between UPF1 and STRAP might indicate a functional connection between these two proteins. While we were unable to test a potential role of UPF1 in UNR-dependent *c-fos* mRNA stability or internal translation initiation of rhinovirus RNA due to the lack of suitable assays, we tested if STRAP knockdown would affect NMD. Our results revealed no effect of STRAP on NMD, but it should be emphasized that negative results of knockdown experiments are as a matter of principle not conclusive. Further work is therefore needed to elucidate the biological role of the UPF1:STRAP interaction.

Another of the newly identified UPF1 interactors in this study, the TREX complex that preferentially associated with pUPF1, is also interesting for several reasons. Human TREX was shown to associate with mRNA during the late steps of splicing and could not be detected on unspliced nascent transcripts.[48] Similarly, in our recent transcriptome-wide mapping of UPF1 binding sites, we found UPF1 almost exclusively associated with exonic sequences and highly underrepresented on introns, rRNA or tRNA.[34] The interaction of pUPF1 with TREX therefore suggests that UPF1 might be recruited to mRNA together with TREX during splicing. The interaction of pUPF1 with TREX and several other nuclear proteins is also intriguing because it is well-documented that NMD is tightly linked to translation and hence assumed to occur in the cytoplasm, and the SMG1-mediated phosphorylation of UPF1 is thought to occur at a late step of the process after recognition of the aberrant translation termination event.[2,3] According to this model, one would expect the small fraction of pUPF1 to reside in the cytoplasm. However, our identification of predominantly nuclear proteins as interactors of pUPF1 challenges this view (Figure 4D) and rather indicates that the small population of nuclear UPF1 seen in immunostainings might correspond the biochemically detected small fraction of pUPF1. Further experiments are needed to test this provocative hypothesis.

Not only are the identified p-UPF1 interactors predominantly nuclear factors, most of them are also known RNA-binding proteins, and accordingly, their association with pUPF1 is in most cases RNA-mediated (Figure 4E). This finding strongly suggests that a majority − if not all − of pUPF1 is bound to RNA. Consistent with this notion, ATPase-deficient UPF1 mutants, which fail to disassemble the NMD complex from the targeted mRNA,[20] accumulate in a hyper-phosphorylated form.[19,38,66]

In summary, the UPF1 interactome exposed by our mass-spectrometry-based approach gives valuable information about UPF1's phosphorylation and RNA-binding status in the nucleus and supports the idea of UPF1 recruitment to mRNA and phosphorylation of UPF1 taking place before translation, possibly even before the mRNP exits the nucleus. After export to the cytoplasm, elongating ribosomes then displace UPF1 from the coding sequence[34] and aberrantly terminating ribosomes either promote the recruitment of RNA decay factors to pUPF1 or properly terminating ribosomes inactivate the remaining pUPF1 by promoting its dephosphorylation. The

dx.doi.org/10.1021/pr5002143 | J. Proteome Res. XXXX, XXX, XXX−XXX

distinction between these two scenarios clearly necessitates further investigations. The detailed characterization of the UPF1-interacting proteins presented herein will facilitate deciphering UPF1's diverse functions in the future.

■ ASSOCIATED CONTENT

Supporting Information

Contains Figure S1: Test of incorporation of heavy amino acids; Figure S2: Scatter plot of peptide intensities of both peptide competition replicates; Figure S3: Western blot assessing UPF1 phosphorylation after treating the cells with okadaic acid; Supplemental Material: Sequences of peptides, qPCR assays, and knockdown targets; Table S1: Master list with primary primary data from all SILAC experiments; Table S2: List of proteins detected in the peptide competition SILAC experiments; Table S3: List of proteins detected in the SILAC experiments with and without RNase A treatment; Table S4: Interactors of UPF1 whose co-purification was sensitive to RNase A treatment of the cell lysates; Table S5: Log2(H/L) ratios of the identified eIF3 subunits in the different SILAC experiments; Table S6: List of proteins detected in the phospho-UPF1 SILAC experiments. This material is available free of charge via the Internet at http://pubs.acs.org.

■ AUTHOR INFORMATION

Corresponding Author

*E-mail: oliver.muehlemann@dcb.unibe.ch.

Present Address

§V.F.: Friedrich Miescher Institute for Biomedical Research, Novartis Research Foundation, Basel, Switzerland.

Notes

The authors declare no competing financial interest.

■ ACKNOWLEDGMENTS

We are grateful to J. Lykke-Andersen (UCSD, U.S.A.), U. Fischer (Univ. of Würzburg, Germany), and W. Keller (Biozentrum Basel, Switzerland) for providing antibodies. This work has been financed by funds from the European Research Council (ERC-StG 207419), the Swiss National Science Foundation (31003A-127614 and −143717), and the canton Bern to O.M. and by funds from Associazione Italiana per la Ricerca sul Cancro AIRC (Special Program Molecular Clinical Oncology −5 per mille #9965) to A.B.

■ REFERENCES

(1) Jankowsky, E. RNA helicases at work: binding and rearranging. *Trends Biochem. Sci.* **2011**, *36* (1), 19−29.

(2) Kervestin, S.; Jacobson, A. NMD: a multifaceted response to premature translational termination. *Nat. Rev. Mol. Cell Biol.* **2012**, *13* (11), 700−712.

(3) Schweingruber, C.; Rufener, S. C.; Zund, D.; Yamashita, A.; Muhlemann, O. Nonsense-mediated mRNA decay - Mechanisms of substrate mRNA recognition and degradation in mammalian cells. *Biochim. Biophys. Acta* **2013**, *1829* (6−7), 612−623.

(4) Muhlemann, O.; Jensen, T. H. mRNP quality control goes regulatory. *Trends Genet.* **2012**, *28* (2), 70−77.

(5) Culbertson, M. R.; Leeds, P. F. Looking at mRNA decay pathways through the window of molecular evolution. *Curr. Opin. Genet. Dev.* **2003**, *13* (2), 207−214.

(6) Chamieh, H.; Ballut, L.; Bonneau, F.; Le Hir, H. NMD factors UPF2 and UPF3 bridge UPF1 to the exon junction complex and stimulate its RNA helicase activity. *Nat. Struct. Mol. Biol.* **2008**, *15* (1), 85−93.

(7) Arias-Palomo, E.; Yamashita, A.; Fernandez, I. S.; Nunez-Ramirez, R.; Bamba, Y.; Izumi, N.; Ohno, S.; Llorca, O. The nonsense-mediated mRNA decay SMG-1 kinase is regulated by large-scale conformational changes controlled by SMG-8. *Genes Dev.* **2011**, *25* (2), 153−164.

(8) Yamashita, A.; Izumi, N.; Kashima, I.; Ohnishi, T.; Saari, B.; Katsuhata, Y.; Muramatsu, R.; Morita, T.; Iwamatsu, A.; Hachiya, T.; Kurata, R.; Hirano, H.; Anderson, P.; Ohno, S. SMG-8 and SMG-9, two novel subunits of the SMG-1 complex, regulate remodeling of the mRNA surveillance complex during nonsense-mediated mRNA decay. *Genes Dev.* **2009**, *23* (9), 1091−1105.

(9) Yamashita, A.; Ohnishi, T.; Kashima, I.; Taya, Y.; Ohno, S. Human SMG-1, a novel phosphatidylinositol 3-kinase-related protein kinase, associates with components of the mRNA surveillance complex and is involved in the regulation of nonsense-mediated mRNA decay. *Genes Dev.* **2001**, *15* (17), 2215−2228.

(10) Anders, K. R.; Grimson, A.; Anderson, P. SMG-5, required for C.elegans nonsense-mediated mRNA decay, associates with SMG-2 and protein phosphatase 2A. *EMBO J.* **2003**, *22* (3), 641−650.

(11) Ohnishi, T.; Yamashita, A.; Kashima, I.; Schell, T.; Anders, K. R.; Grimson, A.; Hachiya, T.; Hentze, M. W.; Anderson, P.; Ohno, S. Phosphorylation of hUPF1 induces formation of mRNA surveillance complexes containing hSMG-5 and hSMG-7. *Mol. Cell* **2003**, *12* (5), 1187−1200.

(12) Okada-Katsuhata, Y.; Yamashita, A.; Kutsuzawa, K.; Izumi, N.; Hirahara, F.; Ohno, S. N- and C-terminal Upf1 phosphorylations create binding platforms for SMG-6 and SMG-5:SMG-7 during NMD. *Nucleic Acids Res.* **2012**, *40* (3), 1251−1266.

(13) Cho, H.; Kim, K. M.; Kim, Y. K. Human proline-rich nuclear receptor coregulatory protein 2 mediates an interaction between mRNA surveillance machinery and decapping complex. *Mol. Cell* **2009**, *33* (1), 75−86.

(14) Unterholzner, L.; Izaurralde, E. SMG7 acts as a molecular link between mRNA surveillance and mRNA decay. *Mol. Cell* **2004**, *16* (4), 587−596.

(15) Jonas, S.; Weichenrieder, O.; Izaurralde, E. An unusual arrangement of two 14−3-3-like domains in the SMG5-SMG7 heterodimer is required for efficient nonsense-mediated mRNA decay. *Genes Dev.* **2013**, *27* (2), 211−225.

(16) Eberle, A. B.; Lykke-Andersen, S.; Muhlemann, O.; Jensen, T. H. SMG6 promotes endonucleolytic cleavage of nonsense mRNA in human cells. *Nat. Struct Mol. Biol.* **2009**, *16* (1), 49−55.

(17) Huntzinger, E.; Kashima, I.; Fauser, M.; Sauliere, J.; Izaurralde, E. SMG6 is the catalytic endonuclease that cleaves mRNAs containing nonsense codons in metazoan. *RNA* **2008**, *14* (12), 2609−2617.

(18) Bhattacharya, A.; Czaplinski, K.; Trifillis, P.; He, F.; Jacobson, A.; Peltz, S. W. Characterization of the biochemical properties of the human Upf1 gene product that is involved in nonsense-mediated mRNA decay. *RNA* **2000**, *6* (9), 1226−1235.

(19) Kashima, I.; Yamashita, A.; Izumi, N.; Kataoka, N.; Morishita, R.; Hoshino, S.; Ohno, M.; Dreyfuss, G.; Ohno, S. Binding of a novel SMG-1-Upf1-eRF1-eRF3 complex (SURF) to the exon junction complex triggers Upf1 phosphorylation and nonsense-mediated mRNA decay. *Genes Dev.* **2006**, *20* (3), 355−367.

(20) Franks, T. M.; Singh, G.; Lykke-Andersen, J. Upf1 ATPase-dependent mRNP disassembly is required for completion of nonsense-mediated mRNA decay. *Cell* **2010**, *143* (6), 938−950.

(21) Isken, O.; Maquat, L. E. The multiple lives of NMD factors: balancing roles in gene and genome regulation. *Nat. Rev. Genet* **2008**, *9*, 699−712.

(22) Kim, Y. K.; Furic, L.; Desgroseillers, L.; Maquat, L. E. Mammalian Staufen1 recruits Upf1 to specific mRNA 3′UTRs so as to elicit mRNA decay. *Cell* **2005**, *120* (2), 195−208.

(23) Kaygun, H.; Marzluff, W. F. Regulated degradation of replication-dependent histone mRNAs requires both ATR and Upf1. *Nat. Struct. Mol. Biol.* **2005**, *12* (9), 794−800.

(24) Chawla, R.; Redon, S.; Raftopoulou, C.; Wischnewski, H.; Gagos, S.; Azzalin, C. M. Human UPF1 interacts with TPP1 and telomerase and sustains telomere leading-strand replication. *EMBO J.* **2011**, *30* (19), 4047−4058.

(25) Azzalin, C. M.; Lingner, J. The human RNA surveillance factor UPF1 is required for S phase progression and genome stability. *Curr. Biol.* **2006**, *16* (4), 433−439.
(26) Ong, S. E.; Blagoev, B.; Kratchmarova, I.; Kristensen, D. B.; Steen, H.; Pandey, A.; Mann, M. Stable isotope labeling by amino acids in cell culture, SILAC, as a simple and accurate approach to expression proteomics. *Mol. Cell. Proteomics* **2002**, *1* (5), 376−386.
(27) Bendall, S. C.; Hughes, C.; Stewart, M. H.; Doble, B.; Bhatia, M.; Lajoie, G. A. Prevention of amino acid conversion in SILAC experiments with embryonic stem cells. *Mol. Cell. Proteomics* **2008**, *7* (9), 1587−1597.
(28) Shevchenko, A.; Tomas, H.; Havlis, J.; Olsen, J. V.; Mann, M. In-gel digestion for mass spectrometric characterization of proteins and proteomes. *Nat. Protoc.* **2006**, *1* (6), 2856−2860.
(29) Rappsilber, J.; Mann, M.; Ishihama, Y. Protocol for micro-purification, enrichment, pre-fractionation and storage of peptides for proteomics using StageTips. *Nat. Protoc.* **2007**, *2* (8), 1896−1906.
(30) Cox, J.; Neuhauser, N.; Michalski, A.; Scheltema, R. A.; Olsen, J. V.; Mann, M. Andromeda: a peptide search engine integrated into the MaxQuant environment. *J. Proteome Res.* **2011**, *10* (4), 1794−1805.
(31) Yepiskoposyan, H.; Aeschimann, F.; Nilsson, D.; Okoniewski, M.; Muhlemann, O. Autoregulation of the nonsense-mediated mRNA decay pathway in human cells. *RNA* **2011**, *17* (12), 2108−2118.
(32) Paillusson, A.; Hirschi, N.; Vallan, C.; Azzalin, C. M.; Muhlemann, O. A GFP-based reporter system to monitor nonsense-mediated mRNA decay. *Nucleic Acids Res.* **2005**, *33* (6), e54.
(33) Buhler, M.; Paillusson, A.; Muhlemann, O. Efficient down-regulation of immunoglobulin mu mRNA with premature translation-termination codons requires the 5′-half of the VDJ exon. *Nucleic Acids Res.* **2004**, *32* (11), 3304−3315.
(34) Zund, D.; Gruber, A. R.; Zavolan, M.; Muhlemann, O. Translation-dependent displacement of UPF1 from coding sequences causes its enrichment in 3′ UTRs. *Nat. Struct Mol. Biol.* **2013**, *20* (8), 936−943.
(35) Hurt, J. A.; Robertson, A. D.; Burge, C. B. Global analyses of UPF1 binding and function reveals expanded scope of nonsense-mediated mRNA decay. *Genome Res.* **2013**, *23*, 1636−1650.
(36) Lykke-Andersen, J.; Shu, M. D.; Steitz, J. A. Human Upf proteins target an mRNA for nonsense-mediated decay when bound downstream of a termination codon. *Cell* **2000**, *103* (7), 1121−1131.
(37) Park, E.; Gleghorn, M. L.; Maquat, L. E. Staufen2 functions in Staufen1-mediated mRNA decay by binding to itself and its paralog and promoting UPF1 helicase but not ATPase activity. *Proc. Natl. Acad. Sci. U. S. A.* **2012**, *110* (2), 405−412.
(38) Isken, O.; Kim, Y. K.; Hosoda, N.; Mayeur, G. L.; Hershey, J. W.; Maquat, L. E. Upf1 phosphorylation triggers translational repression during nonsense-mediated mRNA decay. *Cell* **2008**, *133* (2), 314−327.
(39) Morris, C.; Wittmann, J.; Jack, H. M.; Jalinot, P. Human INT6/eIF3e is required for nonsense-mediated mRNA decay. *EMBO Rep.* **2007**, *8* (6), 596−602.
(40) Peixeiro, I.; Inacio, A.; Barbosa, C.; Silva, A. L.; Liebhaber, S. A.; Romao, L. Interaction of PABPC1 with the translation initiation complex is critical to the NMD resistance of AUG-proximal nonsense mutations. *Nucleic Acids Res.* **2011**, *40* (3), 1160−1173.
(41) Klinge, S.; Voigts-Hoffmann, F.; Leibundgut, M.; Arpagaus, S.; Ban, N. Crystal structure of the eukaryotic 60S ribosomal subunit in complex with initiation factor 6. *Science* **2011**, *334* (6058), 941−948.
(42) Rabl, J.; Leibundgut, M.; Ataide, S. F.; Haag, A.; Ban, N. Crystal structure of the eukaryotic 40S ribosomal subunit in complex with initiation factor 1. *Science* **2010**, *331* (6018), 730−736.
(43) Min, E. E.; Roy, B.; Amrani, N.; He, F.; Jacobson, A. Yeast Upf1 CH domain interacts with Rps26 of the 40S ribosomal subunit. *RNA* **2013**, *19* (8), 1105−1115.
(44) Bardoni, B.; Castets, M.; Huot, M. E.; Schenck, A.; Adinolfi, S.; Corbin, F.; Pastore, A.; Khandjian, E. W.; Mandel, J. L. 82-FIP, a novel FMRP (fragile X mental retardation protein) interacting protein, shows a cell cycle-dependent intracellular localization. *Hum. Mol. Genet.* **2003**, *12* (14), 1689−1698.
(45) Metze, S.; Herzog, V. A.; Ruepp, M. D.; Muhlemann, O. Comparison of EJC-enhanced and EJC-independent NMD in human cells reveals two partially redundant degradation pathways. *RNA* **2013**, 10.1261/rna.038893.113.
(46) Huang, L.; Lou, C. H.; Chan, W.; Shum, E. Y.; Shao, A.; Stone, E.; Karam, R.; Song, H. W.; Wilkinson, M. F. RNA Homeostasis Governed by Cell Type-Specific and Branched Feedback Loops Acting on NMD. *Mol. Cell* **2011**, *43* (6), 950−961.
(47) Antonov, A. V. BioProfiling.de: analytical web portal for high-throughput cell biology. *Nucleic Acids Res.* **2011**, *39* (Web Server issue), W323−W327.
(48) Masuda, S.; Das, R.; Cheng, H.; Hurt, E.; Dorman, N.; Reed, R. Recruitment of the human TREX complex to mRNA during splicing. *Genes Dev.* **2005**, *19* (13), 1512−1517.
(49) Cheng, H.; Dufu, K.; Lee, C. S.; Hsu, J. L.; Dias, A.; Reed, R. Human mRNA export machinery recruited to the 5′ end of mRNA. *Cell* **2006**, *127* (7), 1389−1400.
(50) Katahira, J. mRNA export and the TREX complex. *Biochim. Biophys. Acta* **2012**, *1819* (6), 507−513.
(51) Le Hir, H.; Izaurralde, E.; Maquat, L. E.; Moore, M. J. The spliceosome deposits multiple proteins 20−24 nucleotides upstream of mRNA exon-exon junctions. *EMBO J.* **2000**, *19* (24), 6860−6869.
(52) Steckelberg, A. L.; Boehm, V.; Gromadzka, A. M.; Gehring, N. H. CWC22 Connects Pre-mRNA Splicing and Exon Junction Complex Assembly. *Cell Rep.* **2012**, *2* (3), 454−461.
(53) Barbosa, I.; Haque, N.; Fiorini, F.; Barrandon, C.; Tomasetto, C.; Blanchette, M.; Le Hir, H. Human CWC22 escorts the helicase eIF4AIII to spliceosomes and promotes exon junction complex assembly. *Nat. Struct Mol. Biol.* **2012**, *19* (10), 983−990.
(54) Datta, P. K.; Chytil, A.; Gorska, A. E.; Moses, H. L. Identification of STRAP, a novel WD domain protein in transforming growth factor-beta signaling. *J. Biol. Chem.* **1998**, *273* (52), 34671−34674.
(55) Grimmler, M.; Otter, S.; Peter, C.; Muller, F.; Chari, A.; Fischer, U. Unrip, a factor implicated in cap-independent translation, associates with the cytosolic SMN complex and influences its intracellular localization. *Hum. Mol. Genet.* **2005**, *14* (20), 3099−3111.
(56) Hunt, S. L.; Hsuan, J. J.; Totty, N.; Jackson, R. J. unr, a cellular cytoplasmic RNA-binding protein with five cold-shock domains, is required for internal initiation of translation of human rhinovirus RNA. *Genes Dev.* **1999**, *13* (4), 437−448.
(57) Hosoda, N.; Kim, Y. K.; Lejeune, F.; Maquat, L. E. CBP80 promotes interaction of Upf1 with Upf2 during nonsense-mediated mRNA decay in mammalian cells. *Nat. Struct. Mol. Biol.* **2005**, *12* (10), 893−901.
(58) Hwang, J.; Sato, H.; Tang, Y.; Matsuda, D.; Maquat, L. E. UPF1 association with the cap-binding protein, CBP80, promotes nonsense-mediated mRNA decay at two distinct steps. *Mol. Cell* **2010**, *39* (3), 396−409.
(59) Maquat, L. E.; Tarn, W. Y.; Isken, O. The pioneer round of translation: features and functions. *Cell* **2010**, *142* (3), 368−374.
(60) Rufener, S. C.; Muhlemann, O. eIF4E-bound mRNPs are substrates for nonsense-mediated mRNA decay in mammalian cells. *Nat. Struct. Mol. Biol.* **2013**, *20* (6), 710−717.
(61) Durand, S.; Lykke-Andersen, J. Nonsense-mediated mRNA decay occurs during eIF4F-dependent translation in human cells. *Nat. Struct. Mol. Biol.* **2013**, *20* (6), 702−709.
(62) Zhou, M.; Sandercock, A. M.; Fraser, C. S.; Ridlova, G.; Stephens, E.; Schenauer, M. R.; Yokoi-Fong, T.; Barsky, D.; Leary, J. A.; Hershey, J. W.; Doudna, J. A.; Robinson, C. V. Mass spectrometry reveals modularity and a complete subunit interaction map of the eukaryotic translation factor eIF3. *Proc. Natl. Acad. Sci. U. S. A.* **2008**, *105* (47), 18139−18144.
(63) Choe, J.; Oh, N.; Park, S.; Lee, Y. K.; Song, O. K.; Locker, N.; Chi, S. G.; Kim, Y. K. Translation initiation on mRNAs bound by nuclear cap-binding protein complex CBP80/20 requires interaction between CBP80/20-dependent translation initiation factor and eukaryotic translation initiation factor 3g. *J. Biol. Chem.* **2012**, *287* (22), 18500−18509.

(64) Welch, E. M.; Jacobson, A. An internal open reading frame triggers nonsense-mediated decay of the yeast SPT10 mRNA. *EMBO J.* **1999**, *18* (21), 6134−6145.
(65) Chang, T. C.; Yamashita, A.; Chen, C. Y.; Yamashita, Y.; Zhu, W.; Durdan, S.; Kahvejian, A.; Sonenberg, N.; Shyu, A. B. UNR, a new partner of poly(A)-binding protein, plays a key role in translationally coupled mRNA turnover mediated by the c-fos major coding-region determinant. *Genes Dev.* **2004**, *18* (16), 2010−2023.
(66) Page, M. F.; Carr, B.; Anders, K. R.; Grimson, A.; Anderson, P. SMG-2 is a phosphorylated protein required for mRNA surveillance in Caenorhabditis elegans and related to Upf1p of yeast. *Mol. Cell. Biol.* **1999**, *19* (9), 5943−5951.